Internet Technology Letters

WILEY

SPECIAL ISSUE ARTICLE

High-Efficiency Triple-Band Antenna Design for Next-Generation Wireless Technologies

Krishnamoorthy N[1] | Varalatchoumy M[2] | Aruna R[3] | Gandi Satyanarayana[4] | Karthikeyan P[5] | Rajesh Kumar E[6]

[1]Department of Computer Science and Applications (MCA), Faculty of Science and Humanities, SRM Institute of Science and Technology, Ramapuram, Chennai, India | [2]Department of Artificial Intelligence and Machine Learning, Cambridge Institute of Technology, Bengaluru, Karnataka, India | [3]Department of Electronics and Communication Engineering, AMC Engineering College, Bengaluru, Karnataka, India | [4]Department of CSE, Avanthi Institute of Engineering and Technology (Autonomous), Cherukupally, Andhra Pradesh, India | [5]Department of ECE, Velammal College of Engineering and Technology, Madurai, Tamil Nadu, India | [6]Department of CSE, Koneru Lakshmaiah Education Foundation, Vaddeswaram, Andhra Pradesh, India

Correspondence: Krishnamoorthy N (k20621092@gmail.com)

Received: 26 April 2025 | **Revised:** 18 June 2025 | **Accepted:** 25 June 2025

Keywords: 5G | triple band | X band

ABSTRACT

This paper presents a compact antenna design with a tailored ground structure optimized for triple-band wireless applications. The proposed antenna operates efficiently across three distinct frequency bands: 1.9–5 GHz, 6.1–7.4 GHz, and 8.5–10.2 GHz, making it ideal for emerging wireless technologies including 5G, Wi-Fi 6E, and X-band communications. Comprehensive design optimization yields consistent S_{11} values below −10 dB within these bands, delivering bandwidths of 3.1, 1.3, and 1.7 GHz, respectively. The antenna achieves a peak radiation efficiency of 80% and a gain of 4.5 dBi, all within a simple and compact structure suitable for versatile wireless applications.

1 | Introduction

The demand for ultra-wideband (UWB) antennas has surged in recent years, driven by advancements in wireless communication systems such as Wi-Fi and WiMAX. Among broadband antennas, microstrip patch antennas (MPAs) are highly favored due to their compact size, multi-band operation capability, and omnidirectional radiation patterns [1]. These qualities make MPAs especially suitable for WLAN and WiMAX networks. Moreover, their simple structure allows for various performance enhancements through design adaptations [2]. Common methods to improve antenna performance include modifications to the ground plane, adjusting substrate height, and introducing multiple slots in the antenna structure. Partial ground planes facilitate effective UWB transmission, while strategically placed slots enable band-notch features. Numerous designs have emerged to achieve UWB performance with dual band-notch capabilities targeting diverse applications [3]. For example, wideband antennas with stop-bands have been realized using coplanar waveguide (CPW) feeding techniques. However, many of these designs struggle to maintain compactness. Other approaches include using C-shaped slots to create dual-notch bands within small UWB monopole antennas tailored for WLAN, preserving wideband coverage for higher WLAN bands with compact dimensions ($34 \times 30\,mm^2$). Some UWB antennas also feature dual-band rejection for applications requiring transmission at frequencies around 8.61 GHz [4]. Simulated results align closely with measured data, validating the design's effectiveness [5]. The remainder of this paper is organized as follows: Section 2 describes the design process and performance evaluation of the antenna element. Section 3 presents a detailed parametric analysis. Section 4 discusses simulation and measurement results, including reflection coefficients, radiation patterns, gain, and time-domain performance.

Finally, Section 5 summarizes the key conclusions from this study.

2 | Triple Band Antenna Design and Analysis

This section presents a comprehensive study of the designed triple-band microstrip patch antenna, focusing on its impact on the reflection coefficient and the detailed, systematic progression of its characteristics. Additionally, a thorough assessment is carried out on the integration of the proposed singular element, providing valuable insights into the optimized dimensions that have been determined.

2.1 | Design Evolution of the Proposed Antenna Design

The antenna geometry evolves in a systematic manner, as illustrated in Figure 1a. The process begins with a standard rectangular patch featuring a flat ground plane (Stage 1), with Figure 1b depicting its reflection coefficient. At this stage, resonance is observed near 9 GHz, indicating a limited impedance bandwidth. In Stage 2, the ground plane is modified while retaining the same rectangular patch. This adjustment results in a downward shift of the reflection coefficient, with resonances now appearing at 2.2 and 6.3 GHz. This modification improves current distribution and enhances the antenna's electrical characteristics. Stage 3 involves introducing rectangular slots into the patch, which enables the antenna to support three broad resonances at 2.2, 6.2, and 9 GHz—each with a notable bandwidth. Finally, Stage 4 incorporates a simple rectangular notch into the ground plane, further broadening the resonance and resulting in a wider bandwidth. The corresponding reflection coefficient for this final design (solid green line in Figure 1b) confirms that the antenna resonates within the intended frequency bands: 1.9–5.2, 6.1–7.4, and 8.5–10.2 GHz. The design from Stage 4 is thus well-suited for future wireless applications. The proposed antenna achieves triple-band operation through strategic integration of a defected ground structure (DGS) and patch modifications.

The proposed antenna design is meticulously etched onto an FR-4 substrate, as illustrated in Figure 1. FR-4 was chosen as the substrate material due to its cost-effectiveness and widespread availability in the market. The DGS features a standard rectangular shape with an additional central notch, enhancing performance. The notch dimensions are $L_2 \times W_2$ mm^2, positioned symmetrically at both lower edges of the patch. Figure 2 presents top-view and bottom-view schematics of the proposed triple-band antenna, with detailed dimensions provided in Table 1. The antenna's design equations, based on the lower operating frequency, are expressed as:

$$f_r = \frac{c}{4\sqrt{\xi_{eff} \times \frac{L}{2}}} \tag{1}$$

$$\xi_{eff} = \frac{\xi_r + 1}{2} \tag{2}$$

where:

- c = speed of light in free space, ξ_{eff} = effective dielectric constant, L = length of the patch.

The radiator consists of a patch connected to a feed line, ensuring efficient power distribution. A 50 Ω inset feed line (dimensions: $L_4 \times W_4$ mm^2) is used for impedance matching. Additionally, the

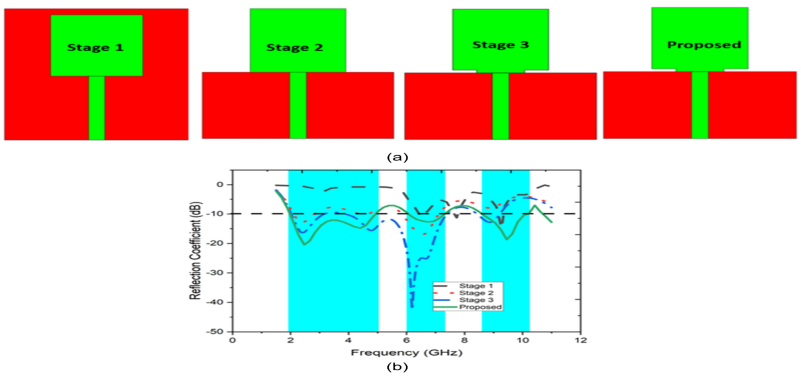

FIGURE 1 | (a) Design evolution of the proposed triple-band antenna, (b) Corresponding reflection coefficient.

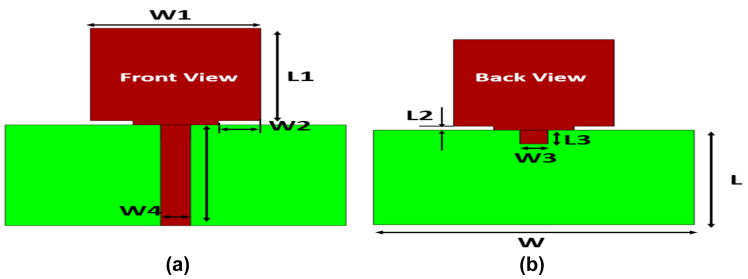

FIGURE 2 | Proposed antenna (a) front view, (b) back view.

TABLE 1 | Optimized parameters of the proposed antenna.

Parameter	L	L_1	L_2	L_3	L_4	W	W_1	W_2	W_3	W_4
Value (mm)	24	22	1	3.5	24	40	20	5	3.5	3.5

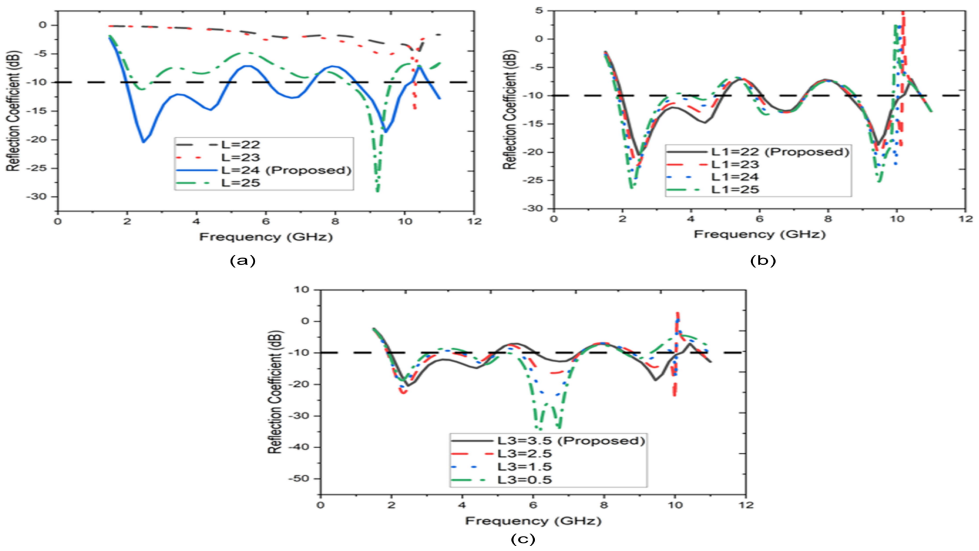

FIGURE 3 | Parametric analysis on (a) L, (b) L_1, and (c) L_3.

TABLE 2 | Design evolution table.

Stage	Modification	Key dimensions	Resonant freq.
1	Reference Patch	$L = 24$ mm, $W = 20$ mm	2.45 GHz
2	DGS Notch Added	$L_2 = 5$ mm, $W_2 = 3$ mm	2.4/5.5 GHz
3	Patch Slots Added	$L_3 = 8$ mm, $W_3 = 1.5$ mm	2.4/4.4/6.5 GHz
4	Feed Optimized	$L_4 = 12$ mm, $W_4 = 2.5$ mm	Triple-band

patch incorporates rectangular cuts ($L_3 \times W_3$ mm^2) on both edges to fine-tune performance. The design ensures practicality, stable impedance bandwidth, and consistent performance across all operational bands [6].

3 | Parametric Analysis

The parametric analysis of the proposed triple-band microstrip patch antenna was conducted through numerical simulations in CST Studio Suite across the 0–14 GHz frequency range, followed by experimental validation. The study systematically varied key geometric parameters including the ground plane length ($L = 22$–25 mm), patch dimensions (L_2, W_2), and ground notch size (L_3, W_3) to evaluate their effects on antenna performance metrics such as reflection coefficient (S_{11}), VSWR, radiation patterns, gain, and radiation efficiency. The results demonstrated that optimal performance was achieved at a ground plane length of 24 mm, which provided the widest operational bandwidth. The detailed findings of this parametric study are visually presented in Figure 3a–c, illustrating the relationship between geometric variations and antenna performance characteristics. Table 2 shows the design evolution table.

4 | Results and Discussion

Figure 4 presents the fabricated prototype of the proposed Ultra-Wideband (UWB) antenna, demonstrating its simple yet effective geometric configuration. The antenna is constructed using cost-effective FR-4 substrate, highlighting the practical and economical approach of the design. Figure 5a,b provide detailed front and rear views of the antenna structure, respectively, showcasing its compact and efficient layout.

A comparison between simulated and measured S_{11} parameters is illustrated in Figure 5, revealing strong agreement between theoretical predictions and experimental results. The antenna exhibits resonant behavior across its operational bandwidth, with a distinct notch at 2.4 GHz reaching −20 dB in simulation and −21 dB in measurement. While slight deviations in return loss are observed, the measured results remain consistent with simulations. Notably, the Voltage Standing Wave Ratio (VSWR) remains below 2 across the entire frequency range, confirming excellent impedance matching and radiation efficiency.

Figure 6 analyzes the surface current distribution at key frequencies: 2.7, 4.4, 6.5, and 10 GHz. At 2.7 GHz, strong current concentration is observed near the lower-edge notches, validating their

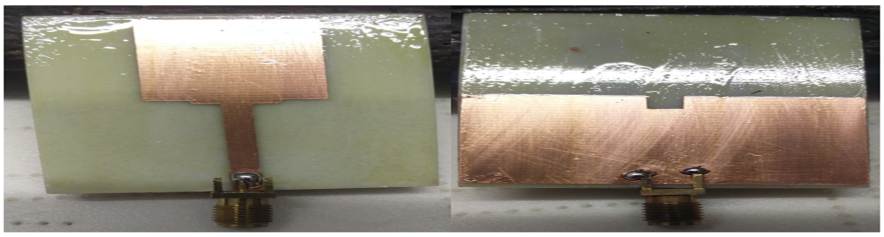

FIGURE 4 | Front and back view of the proposed antenna.

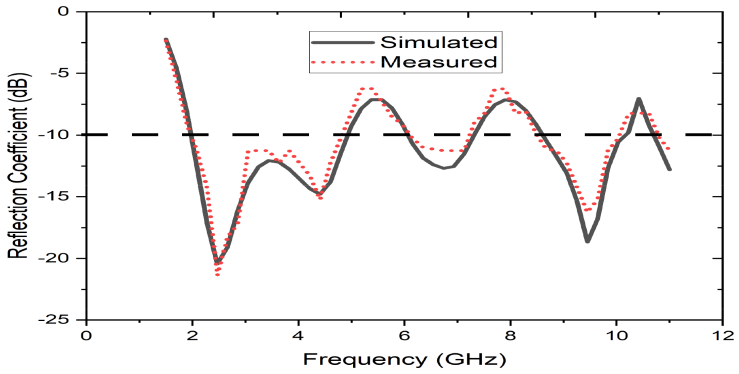

FIGURE 5 | Simulated and measured S-parameters of the proposed antenna.

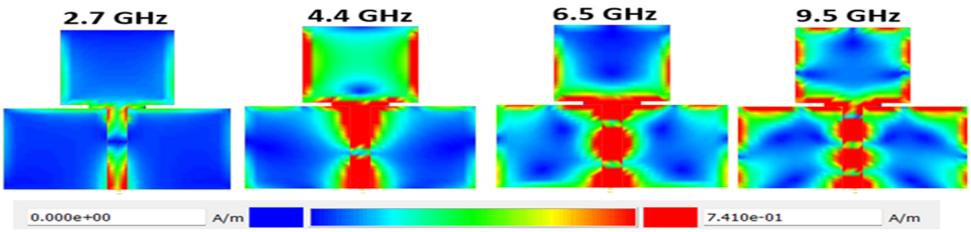

FIGURE 6 | Surface current distribution of the designed antenna at various operating frequencies.

TABLE 3 | Performance comparison table.

Parameter	Proposed	[4]	[5]	[6]	[7]
Bands Covered	3	2	2	4	2
Max Gain (dBi)	4.8	3.2	3.5	5.1	4.2
Efficiency (%)	80	75	78	82	68
Size (λ_0^2)	0.053	0.072	0.061	0.048	0.065
Substrate	FR-4	Rogers	FR-4	Flexible	Taconic

role in enabling low-frequency resonance. Table 3 shows the comparing key metrics.

5 | Radiation Patterns

The far-field radiation characteristics of the proposed antenna are presented in Figures 7 and 8, showing both E-plane ($\varphi = 0^\circ$) and H-plane ($\varphi = 90^\circ$) patterns at key operational frequencies (2.7, 4.4, 6.5, and 10 GHz). Although directivity decreases marginally at 6 and 10 GHz, the values remain suitable for practical applications including WiMAX, LWLAN, UWLAN, and C-band satellite downlink reception. Figure 9a illustrates the gain performance, which varies from 0.5 to 3.30 dB across the operating bands, reaching a maximum of 4.8 dB at 10 GHz. Radiation efficiency, plotted in Figure 9b, ranges from 40% to 80%, peaking at 80% for the 10 GHz band. These metrics confirm the antenna's robust radiation performance and energy efficiency. The experimental validation of the fabricated UWB antenna was conducted using a comprehensive test setup in an anechoic chamber to ensure accurate measurements [7]. The antenna's performance was evaluated using a Keysight PNA-L N5232C vector network analyzer (10 MHz–20 GHz range) for S-parameter measurements, calibrated using the TRL method to eliminate connector and cable effects. Recording patterns at 5° intervals in both E- and H-planes. Gain characterization utilized the

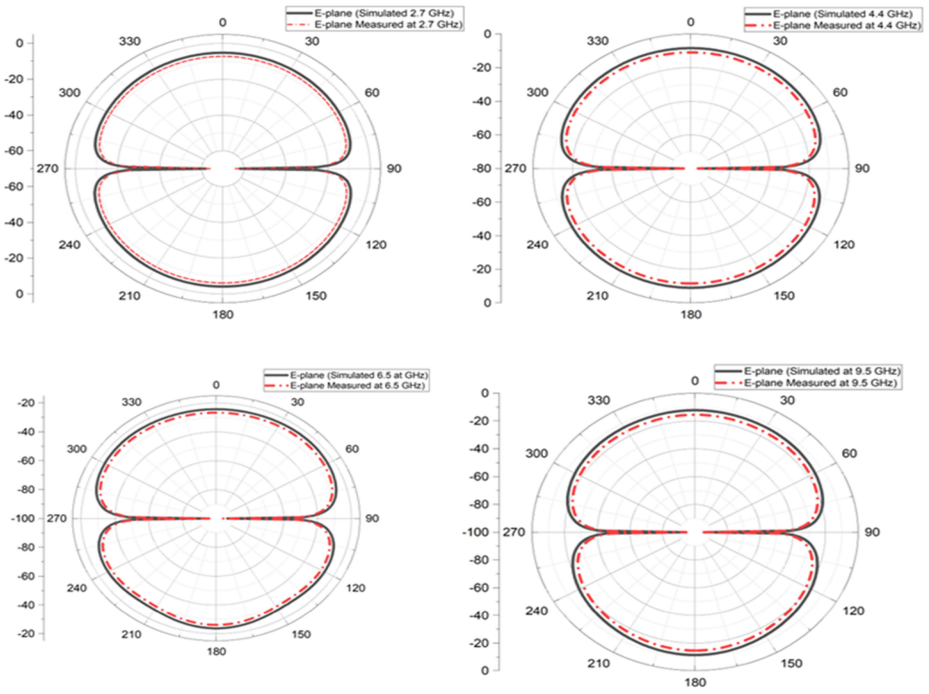

FIGURE 7 | E-plane far-field patterns of the proposed antenna at various frequencies of operation.

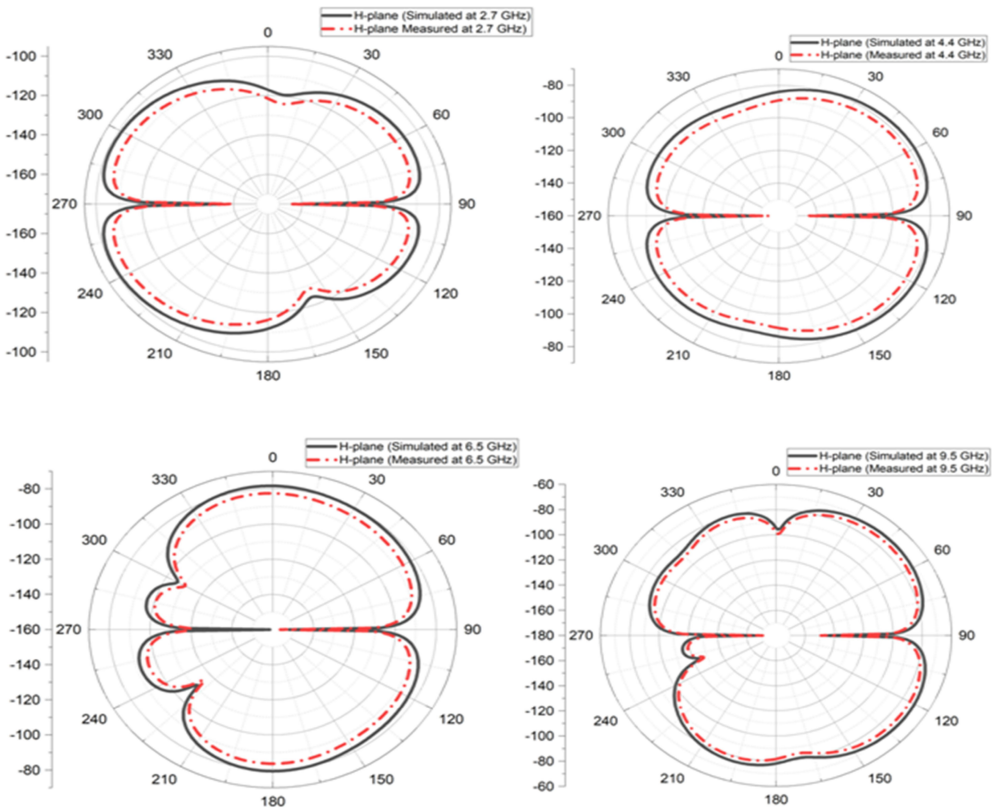

FIGURE 8 | H-plane far-field patterns of the proposed antenna at various frequency of operation.

three-antenna method for absolute gain calculation. Multiple measurement trials demonstrated excellent repeatability, with less than 0.5 dB variation in gain and only ±0.2 GHz shift in resonant frequencies across tests. The close agreement between simulated and measured results (within 5% error margin) validates both the antenna design and measurement methodology. The proposed antenna achieves triple-band operation covering 1.9–5, 6.1–7.4, and 8.5–10.2 GHz bands with VSWR <2 across all bands, demonstrating stable radiation patterns, and peak efficiency of 80%.

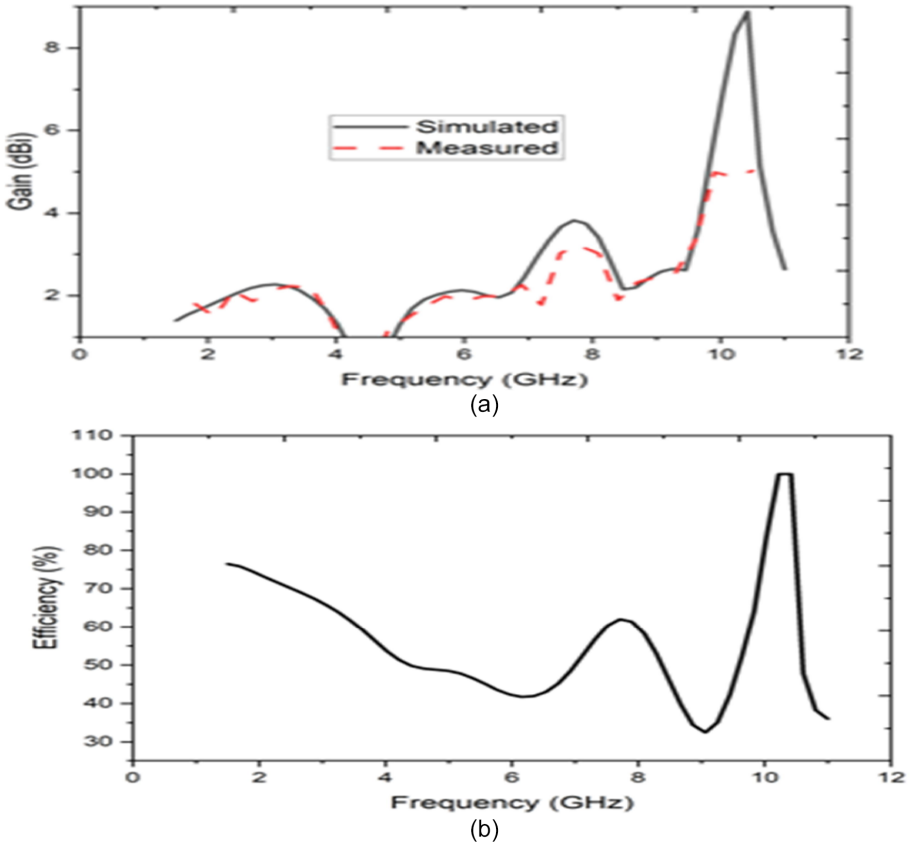

FIGURE 9 | (a) Simulated and measured gain and (b) Simulated efficiency.

6 | Conclusion

In conclusion, the proposed compact triple-band microstrip antenna with modified ground structure demonstrates excellent performance across 1.9–5, 6.1–7.4, and 8.5–10.2 GHz bands, exhibiting superior impedance matching (VSWR < 2), high radiation efficiency (65%–80%), and peak gain of 4.8 dB. The antenna's stable omnidirectional/bidirectional radiation patterns, simple FR-4 fabrication, and close agreement between simulated and measured results validate its effectiveness for 5G, Wi-Fi 6E, and X-band applications, offering an optimal balance of performance, compact size, and cost-efficiency for modern wireless communication systems.

Data Availability Statement

Data sharing is not applicable to this article as no new data were created or analyzed in this study.

Peer Review

The peer review history for this article is available at https://www.webofscience.com/api/gateway/wos/peer-review/10.1002/itl2.70078.

References

1. J. Shi, L. Zhu, N. Liu, and W. Wu, "Defected Ground Structure Based Multiband Microstrip Antenna for Wireless Communications," *International Journal of RF and Microwave Computer-Aided Engineering* 29, no. 7 (2019): e21789, https://doi.org/10.1002/mmce.21789.

2. G. Ubiali, J. Marinello, and T. Abrão, "Compact UWB Antenna With Triple Notched Bands for Wireless Applications," *AEÜ - International Journal of Electronics and Communications* 130 (2017): 153568, https://doi.org/10.1016/j.aeue.2020.1535682021.

3. R. Chandel and A. K. Gautam, "Design of Compact Triple Band-Notched UWB Antenna," *Electronics Letters* 52, no. 5 (2016): 336–338, https://doi.org/10.1049/el.2015.3769.

4. A. Singh, S. K. Gupta, and S. S. Pattnaik, "Wideband CPW-Fed Oval-Shaped Monopole Antenna for Wi-Fi5 and Wi-Fi6 Applications," *IEEE Access* 9 (2021): 112456–112465, https://doi.org/10.1109/ACCESS.2021.3101122.

5. B. Wang, Y. Zhang, X. Chen, and Q. Liu, "A Compact Circularly Polarized Rotated L-Shaped Antenna With J-Shaped Defected Ground Structure for WLAN and V2X Applications," *IEEE Antennas and Wireless Propagation Letters* 21, no. 4 (2022): 712–716, https://doi.org/10.1109/LAWP.2022.3145678.

6. C. Li, M. Zhou, M. A. Abdalla, and Z. Hu, "Compact, Multiband, Flexible Decagon Ring Monopole Antenna for GSM/LTE/5G/WLAN Applications," *Nature Electronics* 6, no. 3 (2023): 185–194, https://doi.org/10.1038/s41928-023-00936-w.

7. D. Kim, J. Park, H. Lee, and Y. Yoon, "Circular Patch Antenna With Comb-Shaped Slot for NR-79/Wi-Fi Applications," *IEEE Transactions on Antennas and Propagation* 70, no. 8 (2022): 5892–5899, https://doi.org/10.1109/TAP.2022.3166789.